

Spectral functions and transport coefficients with the FRG

Ralf-Arno Tripolt

In collaboration with:

Chris Jung, Fabian Rennecke, Naoto Tanji,
Lorenz von Smekal, Jochen Wambach, Johannes Weyrich

Hirschegg 2019: From QCD matter to hadrons

Int. Workshop XLVII on Gross Properties of Nuclei and Nuclear Excitations
Hirschegg, Kleinwalsertal, Austria, January 13-19, 2019

Outline

I) Introduction and motivation

II) Theoretical setup

- ▶ Functional Renormalization Group (FRG)
- ▶ QCD effective model
- ▶ Analytic continuation procedure

III) Results

- ▶ Quark and (pseudo-)scalar meson spectral function
- ▶ Shear viscosity and electrical conductivity
- ▶ (Axial-)vector meson spectral functions
- ▶ Electromagnetic spectral function and dilepton rates

IV) Summary and outlook

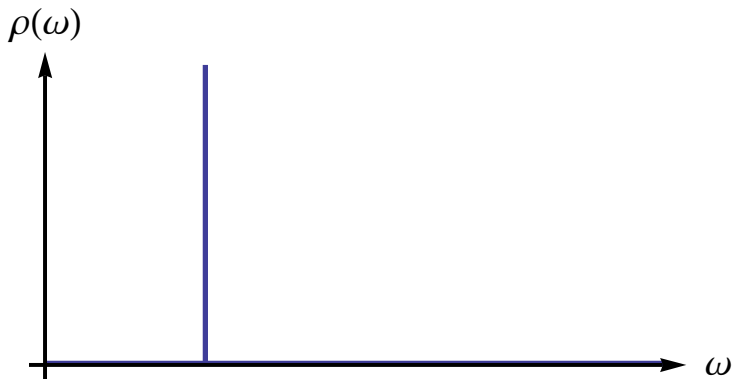
I) Introduction and motivation



[courtesy L. Holicki]

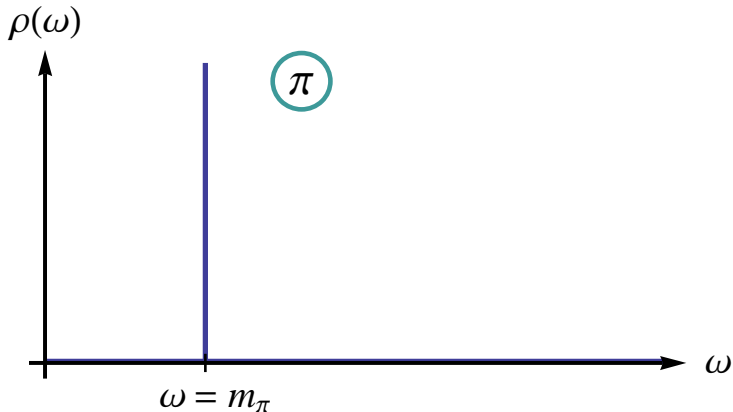
What is a spectral function?

$$\rho(\omega) = -\frac{1}{\pi} \text{Im} D^R(\omega)$$



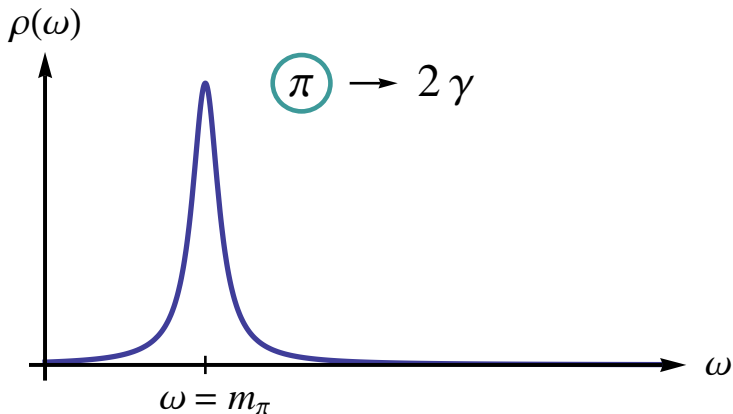
What is a spectral function?

$$\rho(\omega) = -\frac{1}{\pi} \text{Im} D^R(\omega)$$



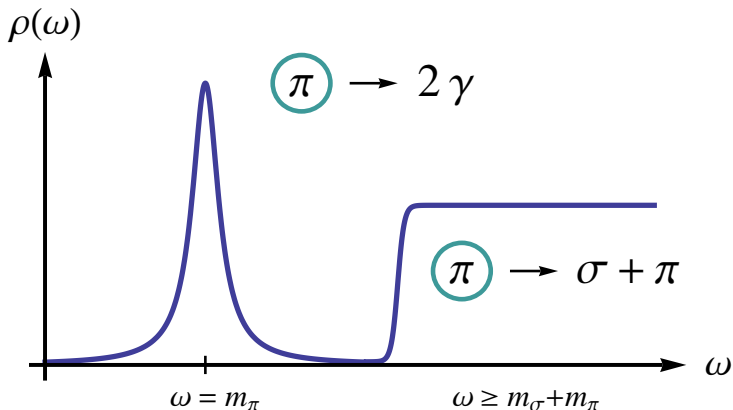
What is a spectral function?

$$\rho(\omega) = -\frac{1}{\pi} \text{Im} D^R(\omega)$$



What is a spectral function?

$$\rho(\omega) = -\frac{1}{\pi} \text{Im} D^R(\omega)$$



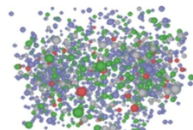
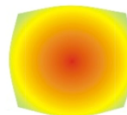
Why are spectral functions interesting?

Spectral functions determine both real-time and imaginary-time propagators,

- ▶ $D^R(\omega) = - \int d\omega' \frac{\rho(\omega')}{\omega' - \omega - i\varepsilon}$
- ▶ $D^A(\omega) = - \int d\omega' \frac{\rho(\omega')}{\omega' - \omega + i\varepsilon}$
- ▶ $D^E(p_0) = \int d\omega' \frac{\rho(\omega')}{\omega' + ip_0}$

and thus allow access to many observables,
e.g. transport coefficients like the shear viscosity:

- ▶ $\eta = \frac{1}{24} \lim_{\omega \rightarrow 0} \lim_{|\vec{p}| \rightarrow 0} \frac{1}{\omega} \int d^4x e^{ipx} \langle [T_{ij}(x), T^{ij}(0)] \rangle$



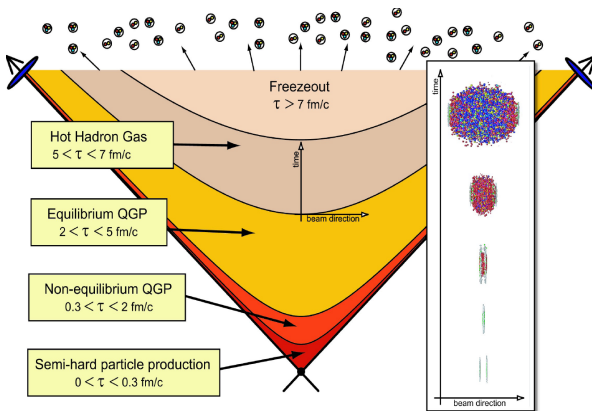
[B. Mueller, arXiv: 1309.7616]

Heavy-ion collisions and electromagnetic probes

compared to the fireball photons and dileptons have a long mean free path

→ leave the interaction zone undisturbed

E. Feinberg 1976, E. Shuryak 1978



[M. Strickland, Acta Phys. Polon. B45 (2014) no.12, 2355-2394]

Dilepton rate and vector meson spectral functions

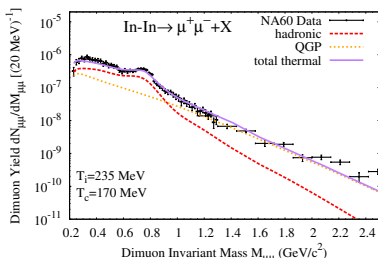
- ▶ Vector mesons ($\rho, \omega, \phi\dots$) can decay directly into lepton pairs
- ▶ Lifetime $\tau_\rho \approx 1.3$ fm/c, smaller than lifetime of fireball (≈ 10 fm/c)

Dilepton rate:

$$\frac{dN_{ll}}{d^4x d^4q} \sim \text{Im} \Pi_{\text{em}}^{\mu\nu}(M, q; \mu, T)$$

For low-energy regime $M \leq 1$ GeV (VMD):

$$\text{Im} \Pi_{\text{em}}^{\mu\nu} \sim \text{Im} D_\rho^{\mu\nu} + \frac{1}{9} \text{Im} D_\omega^{\mu\nu} + \frac{2}{9} \text{Im} D_\phi^{\mu\nu}$$



[Rapp, van Hees, Phys.Lett. B 753 (2016) 586-590]

II) Theoretical setup

$$\begin{aligned}
 S[\psi, \bar{\psi}, A] &= \int d^4x \times \bar{\psi}^{(1)} \left[\gamma_\mu (\partial_\mu + i g A_\mu) + m \right] \psi^{(1)} \rightarrow S[A] = \int d^4x T_{\mu\nu}(\psi) F^{\mu\nu}(A) \\
 \psi(x) \mapsto \psi'(x) &= \Omega(x) \psi(x) \wedge \bar{\psi}'(x) = \bar{\psi} \Omega^\dagger(x) \mapsto S[\psi, \bar{\psi}, A] = S[\psi', \bar{\psi}', A] \cdot S[\Omega, \Omega^\dagger] = m \\
 \Omega^\dagger [\partial_\mu (\Omega \psi)] &= \Omega^\dagger [\partial_\mu \Omega] \psi + \Omega^\dagger (\partial_\mu \psi) = [\partial_\mu \Omega + \Omega^\dagger \Omega \partial_\mu] \psi = [\Omega^\dagger \partial_\mu \Omega + \partial_\mu \Omega^\dagger] \psi \\
 \bar{\psi} \Omega^\dagger (\partial_\mu + i g A_\mu) \Omega \psi &= \bar{\psi} (\partial_\mu + i g A_\mu) \psi \iff S[\partial_\mu (\Omega \psi) + i g A_\mu (\Omega \psi)] = \partial_\mu \psi + i g A_\mu \psi \\
 \Rightarrow S[\partial_\mu \psi] + i g A_\mu \psi &\iff [\Omega^\dagger g A_\mu \Omega] \psi = \partial_\mu \psi + i g A_\mu \psi \quad D_\mu = \partial_\mu - g A_\mu \\
 \Rightarrow A_\mu \rightarrow A'_\mu &= S[\psi] A_\mu + S[\bar{\psi}] \bar{A}_\mu = S[\psi, \bar{\psi}] \Omega^\dagger A_\mu + S[\psi, \bar{\psi}] \Omega A_\mu = S[\psi, \bar{\psi}] \cdot D_\mu = S[\psi, \bar{\psi}] A_\mu \\
 D_\mu \rightarrow D'_{\mu\nu} &= \partial_\mu + i g A_\mu = \partial_\mu + i g S[\psi, \bar{\psi}] A_\mu = \partial_\mu + i g S[\psi, \bar{\psi}] D_\nu = \partial_\mu + i g S[\psi, \bar{\psi}] D_\nu = \partial_\mu + i g S[\psi, \bar{\psi}] A_\nu \\
 F_{\mu\nu} &\rightarrow F'_{\mu\nu} = S[\psi] F_{\mu\nu} + S[\bar{\psi}] \bar{F}_{\mu\nu} = \int d^4x T_{\mu\nu}(\psi) F^{\mu\nu}(A) + \int d^4x T_{\mu\nu}(\bar{\psi}) \bar{F}^{\mu\nu}(A) = A = S[\psi, \bar{\psi}] A
 \end{aligned}$$


[courtesy L. Holicki]

Consistent theoretical framework

How are in-medium modifications of hadrons related to the change of the vacuum structure of QCD? (deconfinement and chiral symmetry restoration,...)

→ want a theoretical framework for computing the thermodynamic and the spectral properties (analytic continuation) of QCD matter on the **same footing!**

Requirements:

- ▶ thermodynamic consistency
- ▶ preservation of symmetries and their breaking pattern

Candidates:

- ▶ mean-field theory
- ▶ Functional Renormalization Group (FRG)
- ▶ ...

FRG includes both **thermal** and **quantum** fluctuations and hence properly deals with phase transitions!

Functional Renormalization Group

Euclidean partition function for a scalar field:

$$Z[J] = \int \mathcal{D}\varphi \exp \left(-S[\varphi] + \int d^4x J(x)\varphi(x) \right)$$

Wilson's coarse-graining: split φ into low- and high-frequency modes

$$\varphi(x) = \varphi_{q \leq k}(x) + \varphi_{q > k}(x)$$

only include fluctuations with $q > k$

$$Z[J] = \underbrace{\int \mathcal{D}\varphi_{q \leq k} \int \mathcal{D}\varphi_{q > k} \exp \left(-S[\varphi] + \int d^4x J(x)\varphi(x) \right)}_{Z_k[J]}$$

Functional Renormalization Group

Scale-dependent partition function can be defined as

$$Z_k[J] = \int \mathcal{D}\varphi \exp \left(-S[\varphi] - \Delta S_k[\varphi] + \int d^4x J(x)\varphi(x) \right)$$

by introducing a regulator term that suppresses IR modes

$$\Delta S_k[\varphi] = \frac{1}{2} \int \frac{d^4q}{(2\pi)^4} \varphi(-q) R_k(q) \varphi(q)$$

Switch to scale-dependent effective action ($\phi(x) = \langle \varphi(x) \rangle$):

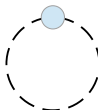
$$\Gamma_k[\phi] = \sup_J \left(\int d^4x J(x)\phi(x) - \log Z_k[J] \right) - \Delta S_k[\phi]$$

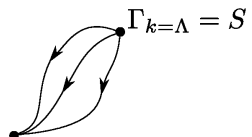
Functional Renormalization Group

Flow equation for the effective average action Γ_k :

$$\partial_k \Gamma_k = \frac{1}{2} S \text{Tr} \left(\partial_k R_k \left[\Gamma_k^{(2)} + R_k \right]^{-1} \right)$$

[C. Wetterich, Phys. Lett. **B 301** (1993) 90]

$$\partial_k \Gamma_k = \frac{1}{2} \text{Tr} \left(\text{Regulator} \right)$$




$$\Gamma_{k=0} = \Gamma$$

[wikipedia.org/wiki/Functional_renormalization_group]

- ▶ Γ_k interpolates between bare action S at $k = \Lambda$ and effective action Γ at $k = 0$
- ▶ regulator R_k acts as a mass term and suppresses fluctuations with momenta smaller than k
- ▶ the use of 3D regulators allows for a simple analytic continuation procedure

Gauged linear-sigma model with quarks

- ▶ $SU(2)_L \times SU(2)_R$: corresponds to chiral symmetry of two-flavor QCD
- ▶ Additional gauge symmetry $U(1)$ to include photon field

Ansatz for the effective average action $\Gamma_k \equiv \Gamma_k[\sigma, \pi, \rho, a_1, \psi, \bar{\psi}, A_\mu]$:

$$\begin{aligned}\Gamma_k = \int d^4x \left\{ & \bar{\psi} (\not{D} - \mu \gamma_0 + h_S (\sigma + i \vec{\tau} \vec{\pi} \gamma_5) + i h_V (\gamma_\mu \vec{\tau} \vec{\rho}^\mu + \gamma_\mu \gamma_5 \vec{\tau} \vec{a}_1^\mu)) \psi + U_k(\phi^2) \right. \\ & \left. - c \sigma + \frac{1}{2} |(D_\mu - ig V_\mu) \Phi|^2 + \frac{1}{8} \text{Tr}(V_{\mu\nu} V^{\mu\nu}) + \frac{1}{4} m_{V,k}^2 \text{Tr}(V_\mu V^\mu) \right\}\end{aligned}$$

with

$$\begin{aligned}V_{\mu\nu} &= D_\mu V_\nu - D_\nu V_\mu - ig [V_\mu, V_\nu], \quad D_\mu \psi = (\partial_\mu - ie A_\mu Q) \psi, \\ D_\mu V_\mu &= \partial_\mu V_\nu - ie A_\mu [T_3, V_\nu], \quad \phi \equiv (\vec{\pi}, \sigma), \quad V_\mu \equiv \vec{\rho}_\mu \vec{T} + \vec{a}_{1,\mu} \vec{T}^5\end{aligned}$$

Flow of the effective potential at $\mu = 0$ and $T = 0$

(Loading movie...)

Flow equations for two-point functions

$$\begin{aligned}\partial_k \Gamma_{k,\psi}^{(2)} &= \text{Diagram 1} + \text{Diagram 2} + 3 \text{Diagram 3} + 3 \text{Diagram 4} \\ \partial_k \Gamma_{k,\sigma}^{(2)} &= \text{Diagram 5} + 3 \text{Diagram 6} - 2 \text{Diagram 7} - \frac{1}{2} \text{Diagram 8} - \frac{3}{2} \text{Diagram 9} \\ \partial_k \Gamma_{k,\pi}^{(2)} &= \text{Diagram 10} + \text{Diagram 11} - 2 \text{Diagram 12} - \frac{1}{2} \text{Diagram 13} - \frac{5}{2} \text{Diagram 14}\end{aligned}$$

The diagrams are circular loop diagrams representing one-loop contributions to the two-point function. They consist of a dashed circle with internal lines connecting vertices. The vertices are labeled with quark ($\psi, \bar{\psi}$) or meson (σ, π) fields and their derivatives. The diagrams are color-coded: blue for quarks, red for mesons, and black for derivatives.

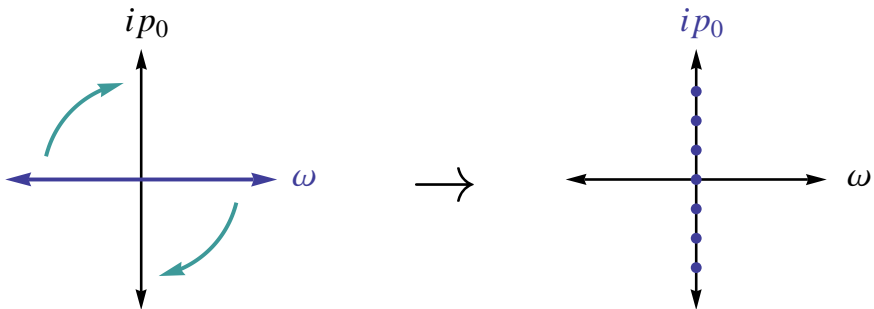
- Diagram 1: A dashed circle with a blue dot at the top. Two blue arrows point clockwise from the left and right towards the dot. Two red arrows point clockwise from the top and bottom away from the dot.
- Diagram 2: A dashed circle with a red dot at the top. Two blue arrows point clockwise from the left and right towards the dot. Two red arrows point clockwise from the top and bottom away from the dot.
- Diagram 3: A dashed circle with a blue dot at the top. Two blue arrows point clockwise from the left and right towards the dot. Two red arrows point clockwise from the top and bottom away from the dot. There is a horizontal line with a blue arrow pointing right and a red arrow pointing left passing through the center.
- Diagram 4: A dashed circle with a red dot at the top. Two blue arrows point clockwise from the left and right towards the dot. Two red arrows point clockwise from the top and bottom away from the dot. There is a horizontal line with a blue arrow pointing right and a red arrow pointing left passing through the center.
- Diagram 5: A dashed circle with a blue dot at the top-left. Two blue arrows point clockwise from the left and right towards the dot. Two red arrows point clockwise from the top and bottom away from the dot.
- Diagram 6: A dashed circle with a blue dot at the top-left. Two blue arrows point clockwise from the left and right towards the dot. Two red arrows point clockwise from the top and bottom away from the dot. There is a horizontal line with a blue arrow pointing right and a red arrow pointing left passing through the center.
- Diagram 7: A dashed circle with a blue dot at the top. Two blue arrows point clockwise from the left and right towards the dot. Two red arrows point clockwise from the top and bottom away from the dot. There is a vertical line with a blue arrow pointing down and a red arrow pointing up passing through the center.
- Diagram 8: A dashed circle with a blue dot at the top. Two blue arrows point clockwise from the left and right towards the dot. Two red arrows point clockwise from the top and bottom away from the dot. There is a vertical line with a blue arrow pointing down and a red arrow pointing up passing through the center. There is also a horizontal line with a blue arrow pointing right and a red arrow pointing left passing through the center.
- Diagram 9: A dashed circle with a blue dot at the top-right. Two blue arrows point clockwise from the left and right towards the dot. Two red arrows point clockwise from the top and bottom away from the dot.
- Diagram 10: A dashed circle with a blue dot at the top-left. Two blue arrows point clockwise from the left and right towards the dot. Two red arrows point clockwise from the top and bottom away from the dot.
- Diagram 11: A dashed circle with a blue dot at the top-left. Two blue arrows point clockwise from the left and right towards the dot. Two red arrows point clockwise from the top and bottom away from the dot. There is a horizontal line with a blue arrow pointing right and a red arrow pointing left passing through the center.
- Diagram 12: A dashed circle with a blue dot at the top. Two blue arrows point clockwise from the left and right towards the dot. Two red arrows point clockwise from the top and bottom away from the dot. There is a vertical line with a blue arrow pointing down and a red arrow pointing up passing through the center.
- Diagram 13: A dashed circle with a blue dot at the top. Two blue arrows point clockwise from the left and right towards the dot. Two red arrows point clockwise from the top and bottom away from the dot. There is a vertical line with a blue arrow pointing down and a red arrow pointing up passing through the center. There is also a horizontal line with a blue arrow pointing right and a red arrow pointing left passing through the center.
- Diagram 14: A dashed circle with a blue dot at the top-right. Two blue arrows point clockwise from the left and right towards the dot. Two red arrows point clockwise from the top and bottom away from the dot.

- quark-meson vertices are given by $\Gamma_{\bar{\psi}\psi\sigma}^{(3)} = h$, $\Gamma_{\bar{\psi}\psi\pi}^{(3)} = ih\gamma^5\vec{\tau}$
- mesonic vertices from scale-dependent effective potential: $U_{k,\phi_i\phi_j\phi_m}^{(3)}$, $U_{k,\phi_i\phi_j\phi_m\phi_n}^{(4)}$
- one-loop structure and 3D regulators allow for a simple analytic continuation!

[R.-A. Tripolt, L. von Smekal, and J. Wambach, Phys. Rev. D 90, 074031 (2014)]

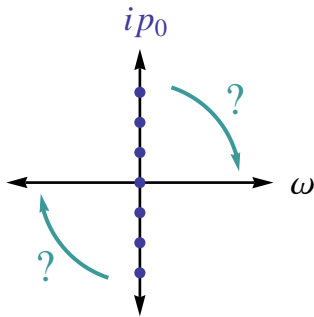
The analytic continuation problem

Calculations at finite temperature are often performed using imaginary energies:



The analytic continuation problem

Analytic continuation problem: How to get back to real energies?



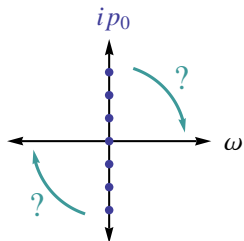
Two-step analytic continuation procedure

1) Use periodicity w.r.t. imaginary energy $ip_0 = i2n\pi T$:

$$n_{B,F}(E + ip_0) \rightarrow n_{B,F}(E)$$

2) Substitute p_0 by continuous real frequency ω :

$$\Gamma^{(2),R}(\omega, \vec{p}) = -\lim_{\epsilon \rightarrow 0} \Gamma^{(2),E}(ip_0 \rightarrow -\omega - i\epsilon, \vec{p})$$



Spectral function is then given by

$$\rho(\omega, \vec{p}) = -\frac{1}{\pi} \text{Im} \frac{1}{\Gamma^{(2),R}(\omega, \vec{p})}$$

[R.-A. T., N. Strodthoff, L. v. Smekal, and J. Wambach, Phys. Rev. D 89, 034010 (2014)]

[J. M. Pawłowski, N. Strodthoff, Phys. Rev. D 92, 094009 (2015)]

[N. Landsman and C. v. Weert, Physics Reports 145, 3&4 (1987) 141]

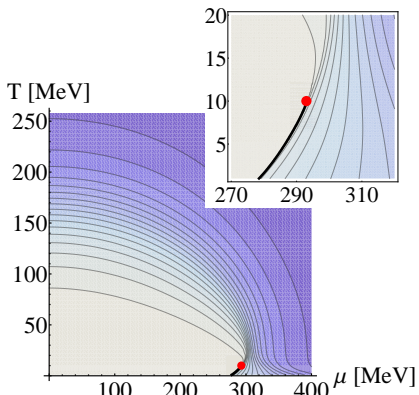
III) Results



[courtesy L. Holicki]

Phase diagram of the quark-meson model

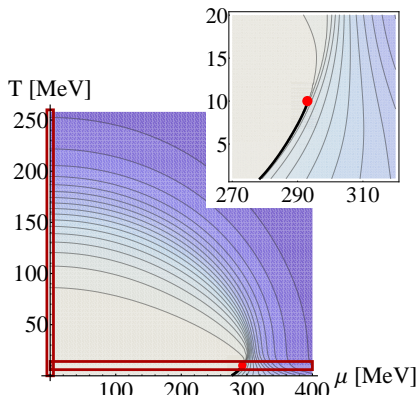
- ▶ chiral order parameter σ_0 decreases towards higher T and μ
- ▶ a crossover is observed at $T \approx 175$ MeV and $\mu = 0$
- ▶ critical endpoint (CEP) at $\mu \approx 292$ MeV and $T \approx 10$ MeV
- ▶ we will study spectral functions along $\mu = 0$ and $T \approx 10$ MeV



[R.-A. T., N. Strodthoff, L. v. Smekal, and J. Wambach, Phys. Rev. D 89, 034010 (2014)]

Phase diagram of the quark-meson model

- ▶ chiral order parameter σ_0 decreases towards higher T and μ
- ▶ a crossover is observed at $T \approx 175$ MeV and $\mu = 0$
- ▶ critical endpoint (CEP) at $\mu \approx 292$ MeV and $T \approx 10$ MeV
- ▶ we will study spectral functions along $\mu = 0$ and $T \approx 10$ MeV



[R.-A. T., N. Strodthoff, L. v. Smekal, and J. Wambach, Phys. Rev. D 89, 034010 (2014)]

Flow of quark spectral function at $\mu = T = 0$

(Loading movie...)

Quark spectral function for $T > 0$

(Loading movie...)

Flow of σ and π spectral function at $\mu = T = 0$

(Loading movie...)

σ and π spectral function for $T > 0$ at $\mu = 0$

(Loading movie...)

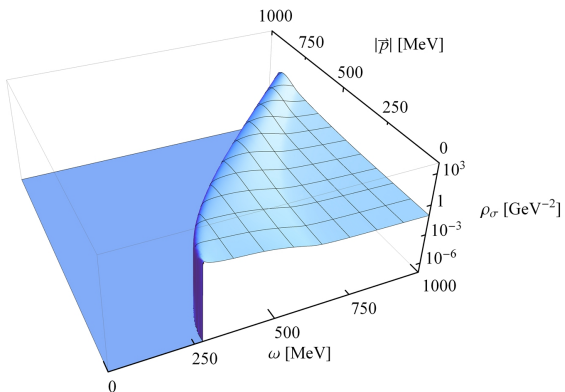
σ and π spectral function for $\mu > 0$ at T_c

(Loading movie...)

σ spectral function vs. ω and \vec{p} at $\mu = T = 0$

T = 0 MeV

- ▶ time-like region
 $(\omega > \vec{p})$ is Lorentz-boosted to higher energies
- ▶ space-like region
 $(\omega < \vec{p})$ is non-zero at finite T due to space-like processes



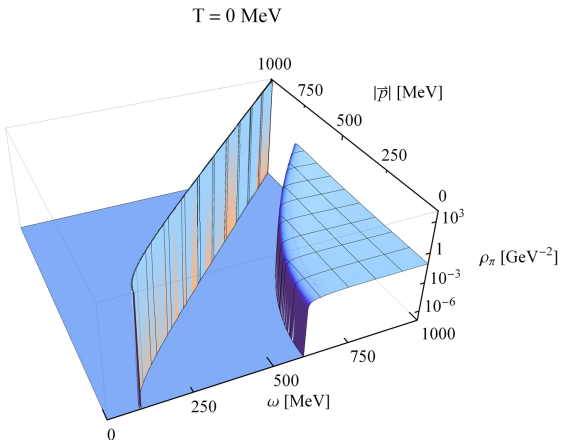
σ spectral function vs. ω and \vec{p} for $T > 0$, $\mu = 0$

- ▶ time-like region
 $(\omega > \vec{p})$ is
Lorentz-boosted to
higher energies
- ▶ space-like region
 $(\omega < \vec{p})$ is non-zero at
finite T due to
space-like processes

(Loading movie...)

π spectral function vs. ω and \vec{p} at $\mu = T = 0$

- ▶ time-like region
 $(\omega > \vec{p})$ is Lorentz-boosted to higher energies
- ▶ capture process
 $\pi^* + \pi \rightarrow \sigma$ is suppressed at large \vec{p}
- ▶ space-like region
 $(\omega < \vec{p})$ is non-zero at finite T due to space-like processes



π spectral function vs. ω and \vec{p} for $T > 0$, $\mu = 0$

- ▶ time-like region
 $(\omega > \vec{p})$ is
Lorentz-boosted to
higher energies
- ▶ capture process
 $\pi^* + \pi \rightarrow \sigma$ is
suppressed at large \vec{p} (Loading movie...)
- ▶ space-like region
 $(\omega < \vec{p})$ is non-zero at
finite T due to
space-like processes

Shear viscosity

Applying the Green-Kubo formula for the shear viscosity

$$\eta = \frac{1}{24} \lim_{\omega \rightarrow 0} \lim_{|\vec{p}| \rightarrow 0} \frac{1}{\omega} \int d^4x e^{ipx} \left\langle [T_{ij}(x), T^{ij}(0)] \right\rangle$$

to the quark-meson model with energy-momentum tensor

$$T^{ij}(x) = \frac{i}{2} \left(\bar{\psi} \gamma^i \partial^j \psi - \partial^j \bar{\psi} \gamma^i \psi \right) + \partial^j \sigma \partial^i \sigma + \partial^j \vec{\pi} \partial^i \vec{\pi}$$

gives

$$\eta_{\sigma,\pi} \propto \int \frac{d\omega}{2\pi} \int \frac{d^3p}{(2\pi)^3} p_x^2 p_y^2 n'_B(\omega) \rho_{\sigma,\pi}^2(\omega, \vec{p})$$

[R.-A. Tripolt, L. von Smekal, and J. Wambach, Int.J.Mod.Phys. E26 (2017) no.01n02, 1740028]

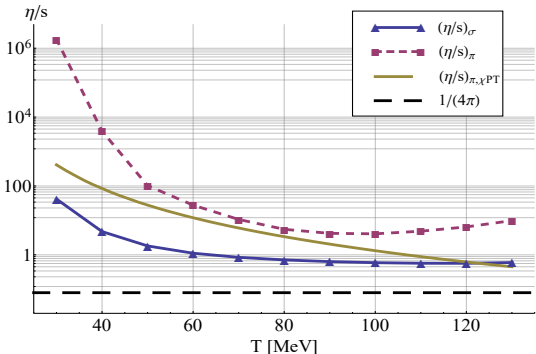
Shear viscosity over entropy density η/s at $\mu=0$

- ▶ $\eta_{\pi,\chi\text{PT}}$: result from chiral perturbation theory

[Lang, Kaiser, Weise, EPJ A 48, 109 (2012)]

- ▶ large shear viscosity at low temperatures due to small width of pion peak
→ 4π processes missing
- ▶ η/s is always larger than the AdS/CFT limiting value of $\eta/s \geq 1/4\pi$

[R.-A. Tripolt, L. von Smekal, and J. Wambach, Int.J.Mod.Phys. E26 (2017) no.01n02, 1740028]



Electrical conductivity

Applying the Green-Kubo formula for the electrical conductivity

$$\sigma_{el} = \frac{1}{6} \lim_{\omega \rightarrow 0} \lim_{|\vec{p}| \rightarrow 0} \frac{1}{\omega} \int d^4x e^{ipx} \left\langle [J_i(x), J^i(0)] \right\rangle$$

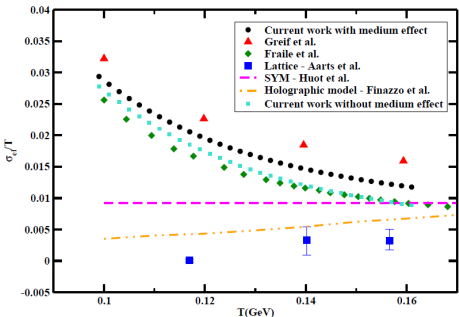
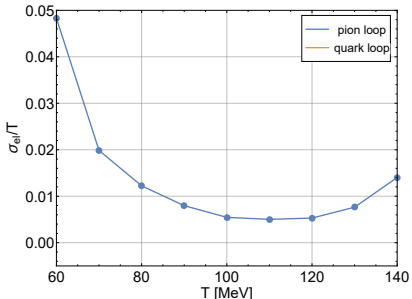
to the quark-meson model with the EM current

$$J^\mu(x) = i \frac{\partial}{\partial A_\mu(x)} \Gamma = e \bar{\psi} \gamma^\mu Q \psi + ie \frac{m_\rho^2}{m_{a_1}^2} (\pi^1 \partial^\mu \pi^2 - \pi^2 \partial^\mu \pi^1) + ie^2 A^\mu [(\pi^1)^2 + (\pi^2)^2]$$

gives

$$\sigma_{el,\pi} \propto \int \frac{d\omega}{2\pi} \int \frac{d^3p}{(2\pi)^3} \vec{p}^2 n'_B(\omega) \rho_\pi^2(\omega, \vec{p})$$

Electrical conductivity vs. T at $\mu = 0$ - Preliminary



[S. Ghosh, S. Mitra, and S. Sarkar, Nucl. Phys. A 969, 237 (2018)]

Flow equations for ρ and a_1 2-point functions

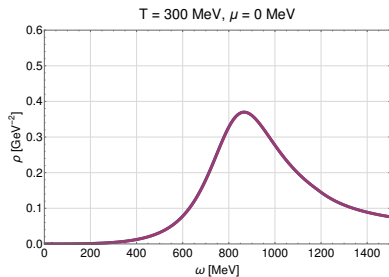
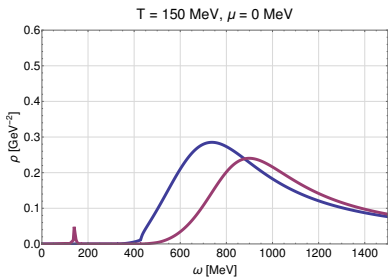
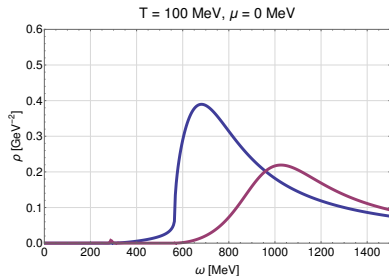
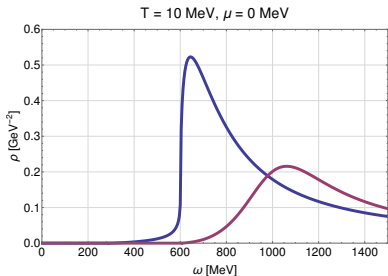
$$\partial_k \Gamma_{\rho,k}^{(2)} = -\frac{1}{2} \left[\text{Diagram 1} + \text{Diagram 2} \right] - 2 \text{Diagram 3}$$

$$\partial_k \Gamma_{a_1,k}^{(2)} = \text{Diagram 4} + \text{Diagram 5} - \frac{1}{2} \left[\text{Diagram 6} + \text{Diagram 7} \right] - 2 \text{Diagram 8}$$

- ▶ neglect vector mesons inside the loops
- ▶ vertices extracted from ansatz for the effective average action Γ_k
- ▶ tadpole diagrams give ω -independent contributions

[C. Jung, F. Rennecke, R.-A. T., L. von Smekal, and J. Wambach, Phys. Rev. D 95, 036020 (2017)]

T -dependence of ρ and a_1 spectral functions



T-dependence of ρ and a_1 spectral functions

(Loading movie...)

Electromagnetic (EM) spectral function

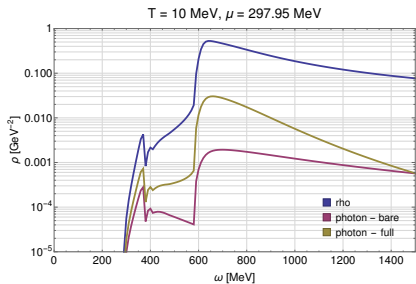
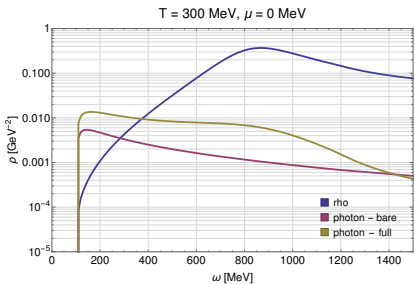
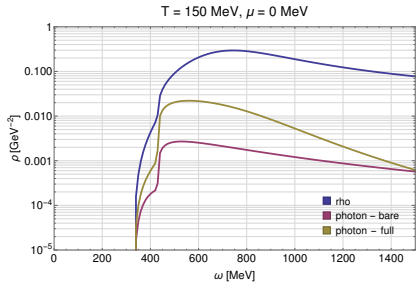
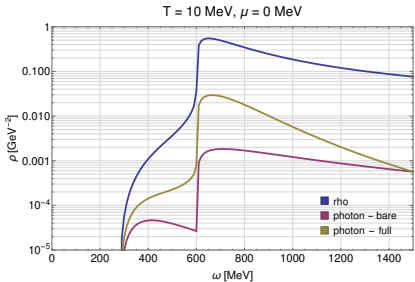
$$\begin{pmatrix} \Gamma_{AA}^{(2)} & \Gamma_{A\rho}^{(2)} \\ \Gamma_{\rho A}^{(2)} & \Gamma_{\rho\rho}^{(2)} \end{pmatrix} \xrightarrow{\text{diagonalize}} \begin{pmatrix} \tilde{\Gamma}_{AA}^{(2)} & 0 \\ 0 & \tilde{\Gamma}_{\rho\rho}^{(2)} \end{pmatrix}, \quad \tilde{\Gamma}_{AA}^{(2)} = \overbrace{\Gamma_{AA}^{(2)} - \frac{\Gamma_{A\rho}^{(2)}\Gamma_{\rho A}^{(2)}}{\Gamma_{\rho\rho}^{(2)}}}^{\mathcal{O}(e^2)} + \mathcal{O}(e^4)$$

$$\partial_k \Gamma_{\rho\rho,k}^{(2)} = \begin{array}{c} \text{Diagram: } \text{---}(\text{---})\text{---} \\ \text{---}(\text{---})\text{---} \\ \text{---}(\text{---})\text{---} \\ \text{---}(\text{---})\text{---} \end{array} - \frac{1}{2} \begin{array}{c} \text{Diagram: } \text{---}(\text{---})\text{---} \\ \text{---}(\text{---})\text{---} \\ \text{---}(\text{---})\text{---} \\ \text{---}(\text{---})\text{---} \end{array} - 2 \begin{array}{c} \text{Diagram: } \text{---}(\text{---})\text{---} \\ \text{---}(\text{---})\text{---} \\ \text{---}(\text{---})\text{---} \\ \text{---}(\text{---})\text{---} \end{array}$$

$$\partial_k \Gamma_{AA,k}^{(2)} = \begin{array}{c} \text{Diagram: } \text{---}(\text{---})\text{---} \\ \text{---}(\text{---})\text{---} \\ \text{---}(\text{---})\text{---} \\ \text{---}(\text{---})\text{---} \end{array} - \frac{1}{2} \begin{array}{c} \text{Diagram: } \text{---}(\text{---})\text{---} \\ \text{---}(\text{---})\text{---} \\ \text{---}(\text{---})\text{---} \\ \text{---}(\text{---})\text{---} \end{array} - 2 \begin{array}{c} \text{Diagram: } \text{---}(\text{---})\text{---} \\ \text{---}(\text{---})\text{---} \\ \text{---}(\text{---})\text{---} \\ \text{---}(\text{---})\text{---} \end{array}$$

$$\partial_k \Gamma_{A\rho,k}^{(2)} = \begin{array}{c} \text{Diagram: } \text{---}(\text{---})\text{---} \\ \text{---}(\text{---})\text{---} \\ \text{---}(\text{---})\text{---} \\ \text{---}(\text{---})\text{---} \end{array} - \frac{1}{2} \begin{array}{c} \text{Diagram: } \text{---}(\text{---})\text{---} \\ \text{---}(\text{---})\text{---} \\ \text{---}(\text{---})\text{---} \\ \text{---}(\text{---})\text{---} \end{array} - 2 \begin{array}{c} \text{Diagram: } \text{---}(\text{---})\text{---} \\ \text{---}(\text{---})\text{---} \\ \text{---}(\text{---})\text{---} \\ \text{---}(\text{---})\text{---} \end{array}$$

EM spectral function - preliminary



Calculation of dilepton rates

- ▶ We use the Weldon formula for the thermal dilepton rate:

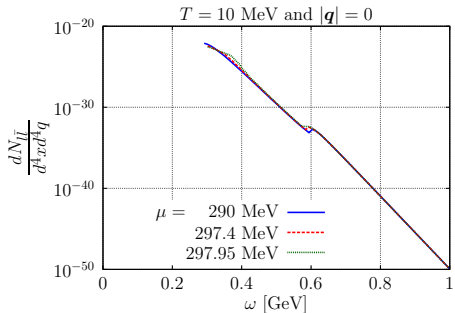
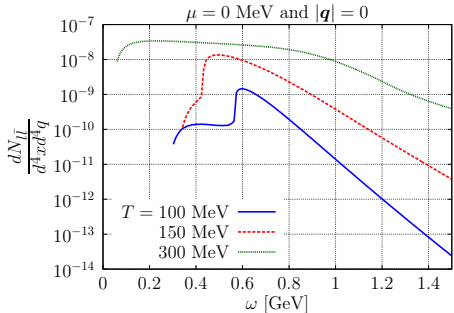
$$\frac{d^8 N_{l\bar{l}}}{d^4 x d^4 q} = \frac{\alpha}{12\pi^3} \left(1 + \frac{2m^2}{q^2}\right) \left(1 - \frac{4m^2}{q^2}\right)^{1/2} q^2 (2\rho_T + \rho_L) n_B(q_0)$$

- ▶ in the following we assume $m = 0$ and set the external spatial momentum to zero, such that $\rho_T = \rho_L = \rho_{\tilde{A}\tilde{A}}$

[H. A. Weldon, Phys. Rev. D42, 2384 (1990)]

[R.-A. T., C. Jung, N. Tanji, L. von Smekal, and J. Wambach, arXiv:1807.04952]

Dilepton rates - preliminary



- ▶ clear changes are visible with increasing temperature
- ▶ no distinct signatures for the critical endpoint yet → improve truncation

[R.-A. T., C. Jung, N. Tanji, L. von Smekal, and J. Wambach, arXiv:1807.04952]

Summary and Outlook

- ▶ analytically continued flow equations for quark and (vector-)meson spectral functions using effective models for QCD within a consistent FRG framework
- ▶ degeneracy of ‘parity partners’ due to restoration of broken chiral symmetry in the QCD medium

Outlook:

- ▶ quark spectral function at finite density and temperature
- ▶ improve truncation (include baryons and more decay channels) to calculate realistic dilepton rates and identify signatures of phase transitions
- ▶ transport coefficients like the shear viscosity and the electrical conductivity